

PROCEEDINGS OF SPIE

SPIEDigitalLibrary.org/conference-proceedings-of-spie

Betatron radiation enhancement by a density up-ramp in the bubble regime of LWFA

Dominika Mašlárová, Vojtěch Horný, Miroslav Krus, Jan Psikal

Dominika Mašlárová, Vojtěch Horný, Miroslav Krus, Jan Psikal, "Betatron radiation enhancement by a density up-ramp in the bubble regime of LWFA," Proc. SPIE 11037, Laser Acceleration of Electrons, Protons, and Ions V, 1103710 (24 April 2019); doi: 10.1117/12.2520980

SPIE.

Event: SPIE Optics + Optoelectronics, 2019, Prague, Czech Republic

Betatron radiation enhancement by a density up-ramp in the bubble regime of LWFA

Dominika Mašlárová^{a,b}, Vojtěch Horný^a, Miroslav Krůš^a, and Jan Pšikal^b

^aInstitute of Plasma Physics, Czech Academy of Sciences, Za Slovankou 3, 182 00 Prague,
Czech Republic

^bCzech Technical University in Prague - FNSPE, Břehová 7, 115 19 Prague, Czech Republic

ABSTRACT

We examine betatron radiation properties from the bubble regime of laser-wakefield acceleration for a tailored plasma density profile. Previous studies have already discussed enhancement of radiation properties by using various density modifications in later acceleration phases. This paper will focus on a density profile with a short linear up-ramp and compare it with a uniform density case. The process is studied for standard parameters feasible with current sub-100 TW laser systems by means of numerical particle-in-cell simulations. We show here that the critical energy and intensity of radiation increase when the plasma density increases. This enhancement is caused either by electron energy gain in the rear part of the bubble or by oscillation amplitude boost by fields behind the bubble.

Keywords: laser-wakefield acceleration, bubble regime, betatron radiation, optical injection, plasma density ramp, particle-in-cell

1. INTRODUCTION

Laser-wakefield acceleration (LWFA) is a promising concept of compact electron accelerators producing ultra-short, coherent synchrotron radiation in the X-ray domain.¹ Radiation in LWFA is emitted by (betatron) oscillations of electrons during the acceleration process.^{2–5} These oscillations are caused by the transverse force experienced by electrons besides the longitudinal accelerating field. Radiation is emitted mostly at the turning points of electron sine-like trajectories.

In the bubble regime of LWFA, ponderomotive force of an intense laser pulse (normalized vector potential $a_0 > 2$) expels plasma electrons radially outward. Consequently, an ion cavity (bubble) is formed behind the pulse. Electrons experience accelerating force at the rear part of the bubble. It is possible to approximate the bubble as a uniformly charged ion sphere⁶ of a radius

$$r_b = 2\sqrt{a_0}/k_p, \quad (1)$$

where k_p is the plasma wavenumber.⁷ The wavelength of betatron oscillations in the bubble is then $\lambda_\beta = \lambda_p \sqrt{2\gamma}$, where λ_p is plasma wavelength and γ is Lorentz factor of the electron.^{2,3} Due to the gradual growth of γ during the acceleration, λ_β also increases. When the electron changes the direction, momentum varies rapidly but the change in energy is small. In this case, the amplitude of oscillations r_β decreases with $\gamma^{-1/4}$.^{8,9} Therefore, these oscillations are damped with time.

Parameter $K = r_\beta k_p \sqrt{\gamma/2}$ is used to distinguish two different regimes of radiation: undulator regime ($K \ll 1$), and wiggler regime ($K \gg 1$) which occurs exclusively.^{5,10–12} In the latter regime, half of the radiation power is emitted at frequencies below the critical frequency $\omega_c = \frac{3}{2} K \gamma^2 \omega_\beta$, where ω_β is the frequency of betatron oscillations. Corresponding critical energy is defined as $E_c = \hbar \omega_c$. It can be easily derived that

$$\omega_c \sim \frac{\sqrt{n} r_\beta \gamma^{5/2}}{\lambda_\beta}. \quad (2)$$

Further author information: (Send correspondence to D. Maslarova)
E-mail: maslarova@ipp.cas.cz

Thus, the critical frequency increases with the increasing density n , electron energy and oscillation amplitude, and decreases with the increasing betatron wavelength.

In recent years, various approaches of radiation enhancement have been proposed, such as interaction of the electron bunch with the rear part of the driving pulse,^{13–15} a tailored profile of the driving pulse,^{12,16} a clustering gas jet target,¹⁷ long focal length optics¹⁸ and double injection in an evolving bubble.¹⁹

Several studies also showed that manipulation with the plasma density is a promising method of enhancing the betatron radiation. Besides transverse density gradients,^{20,21} also modifications in longitudinal density profiles may significantly influence the properties of the final radiation.

For instance, density step down-ramps and up-ramps were examined theoretically.²² In the case of a step down-ramp, the density is reduced for efficiently long time to zero. When electrons enter the depleted region, forces they experience vanish. As a result, electrons drift at the constant energy and angle for a short time. Subsequently, they enter the region of non-zero density with higher r_β , which leads to an increase in ω_c . In the region of a step up-ramp, the bubble is forced to diminish. According to the above mentioned spherical model of the bubble (1), r_b decreases as density increases. As a consequence, the electrons occur again at the rear part of the bubble with larger accelerating field. Such a phase-reset leads to the electron energy gain²³ and the increase in γ . Also, another density depressed structure, between two peaks of high density, was investigated experimentally and by PIC simulations.²⁴ Enhanced betatron radiation was observed, depending mainly on a betatron phase, electron energy and length of the depression.

In order to address previous research, we investigate betatron radiation from an electron bunch propagating in a short linear up-ramp²⁵ here. The main aim is to establish differences in betatron radiation wavelength, amplitude, critical frequency and spectrum compared with uniform density profile.

2. PIC SIMULATIONS

Numerical particle-in-cell simulations were performed using the 2D version of EPOCH code.²⁵ In our simulations, a linearly polarized driving pulse with a Gaussian spatial and temporal profile ($a_0 = 4$, $\lambda_0 = 0.8\mu\text{m}$) propagates in the x -direction. We used a simulation window moving with the group velocity of the pulse. The pulse is focused into a waist of $9.5\mu\text{m}$ and its FWHM duration is 17.6 fs. The size of the simulation box is $85 \times 30\mu\text{m}^2$; the cell size is $0.027 \times 0.04\mu\text{m}^2$ with 4 macroparticles per cell.

The pulse firstly enters a $10\mu\text{m}$ -long density up-ramp and then propagates in the uniform density ($n_0 = 5 \cdot 10^{18}\text{ cm}^{-3}$). After $50\mu\text{m}$ of propagation, the drive pulse collides with a second pulse with perpendicular polarization propagating in the transverse y -direction (OC3P injection²⁶). The second pulse is less intense ($a_0 = 0.4$), while all the other parameters are maintained the same. As a consequence, a bunch of electrons is

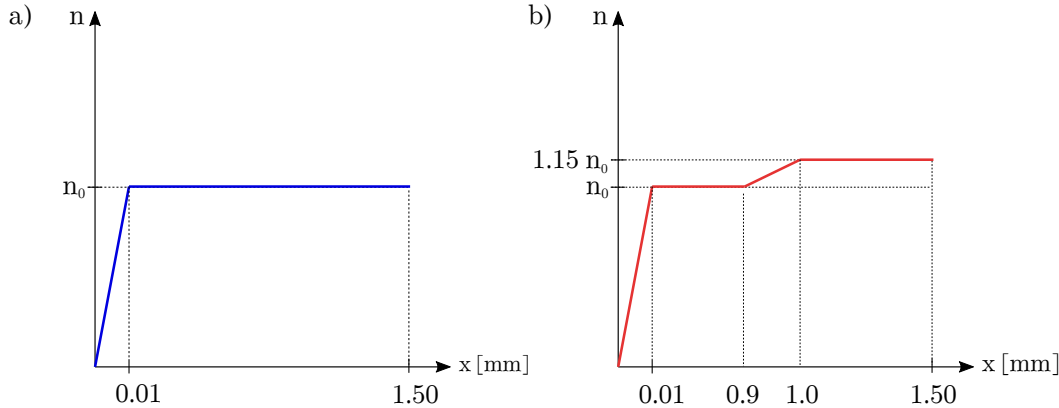


Figure 1: Two density profiles with a short linear up-ramp entrance: a) uniform density n_0 , b) uniform density followed by a 0.1-mm -long linear up-ramp after 0.9 mm of pulse propagation.

injected and trapped in the wakefield. This injection was chosen due to the fact that it does not influence later evolution of fields in the bubble.²⁷

The bunch is further accelerated in the uniform plasma density for 0.9 mm. Afterward, two different cases of density profiles shown in Figure 1 are presented. In the first case, the pulse continues to propagate in the uniform plasma density. In the second case, the density starts to grow linearly until $n = 1.15 n_0$ is reached in 1 mm of the propagation. The choice of this value will be described in the next section. The subsequent evolution of the bunch was studied until 1.5 mm of the propagation.

The betatron spectra were calculated by the code based on the Liénard-Wiechert potentials.²⁸ Position and momentum of accelerated electrons had to be properly sampled in order to capture also a high energy tail of X-ray spectrum. For this purpose, a particle tracker implemented by authors into EPOCH code was used. Five percent of the bunch was chosen as a sample to represent properties of the final radiation. Exactly the same macroparticles were studied for both density cases. In this manner, we were also able to study variations in the single particle radiation.

3. PLASMA DENSITY UP-RAMP

In this section, we briefly discuss how the height of the up-ramp is chosen. From formula (1), it can be seen that the radius of the bubble decreases as the density increases because $k_p \sim n$. Therefore, we expected the shrinkage of the bubble after propagation through the density up-ramp. Corresponding evolution of the radius is shown in Figure 2.

In the case without the up-ramp, the bubble radius gradually increases. In the up-ramp case, the density profile is tailored to compensate the radius growth. We estimated the required increase of the density according to formula (1)²³ in order to push electrons into their original position in the bubble right after the injection (0.15 mm of propagation). In our simulation, the radius of the bubble after 0.15 mm of propagation was $r_{b1} = 10.32 \mu\text{m}$. After 0.9 mm of propagation, $r_{b2} = 11.09 \mu\text{m}$. As a result, we determined that it is required to increase the density $(r_{b2}/r_{b1})^2 \sim 1.15 \times n_0$. Although the radius of the bubble is not constant and evolves through the simulation, the estimation of density up-ramp height by (1) seems to be qualitatively accurate. The radius shrank into its original value after passing through the up-ramp in 1.1 mm of propagation.

4. BETATRON RADIATION

In this section, we show how the properties of the betatron radiation change when a density up-ramp is applied during the acceleration. The energy spectrum and distribution of the bunch are depicted in Figure 3, properties of betatron radiation from the bunch sample are shown in Figure 4; spectrograms are shown in Figure 5. The results are calculated after 1.5 mm of propagation in the plasma and compared to the case without an up-ramp.

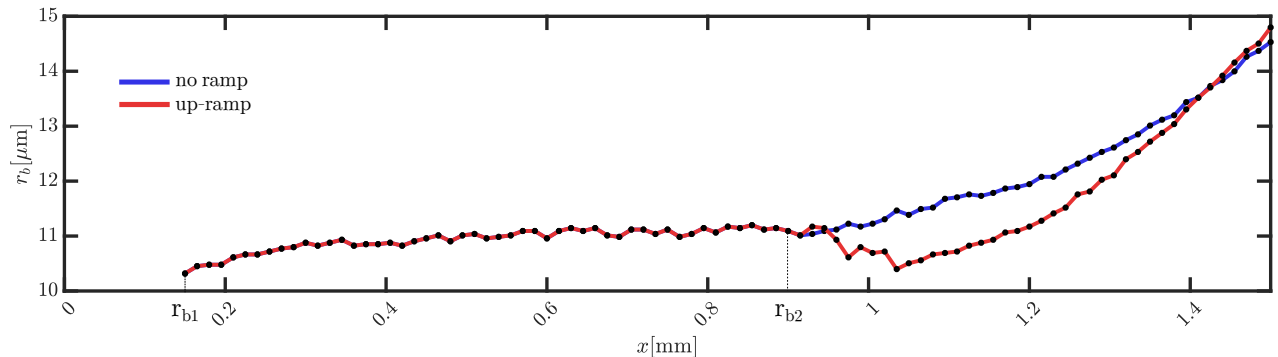


Figure 2: Evolution of a bubble radius during the acceleration for two density profiles: uniform density (blue) and linear up-ramp (red). The radius of the bubble after 0.15 mm of propagation was $r_{b1} = 10.32 \mu\text{m}$. After 0.9 mm of propagation, $r_{b2} = 11.09 \mu\text{m}$.

The most significant difference is in the radiative power and critical frequency. Both these quantities are higher if the bunch propagates through the ramp.

The simulations show that the energy spectrum of the bunch sample is shifted to higher values after propagating through the up-ramp, while maintaining the spectrum shape almost the same. Also, the shape of the betatron radiative power temporal profile does not change; however, the spectral intensity and critical frequency rapidly increase. Three separate pulses of radiation are observed on axis in both cases. The most significant change can be seen in the last pulse observed in 8 fs. Radiative power increased from 2.0 to $5.4 \cdot 10^{-15} \text{ J} \cdot \text{sr}^{-1} \cdot \text{fs}^{-1} \cdot \text{electron}^{-1}$ (12.5 to $33.7 \text{ keV} \cdot \text{sr}^{-1} \cdot \text{fs}^{-1} \cdot \text{electron}^{-1}$). The duration of this X-ray pulse shorten from 1.2 to 0.9 fs. Moreover, a significant increase in the critical energy can be seen after this time, up to almost 540% reached in 9.7 fs.

The results indicate that the increase in the critical frequency (2) is caused by two different reasons, depending on the electron position. Radiation of two example electrons depicted in Figure 7 is shown in order to demonstrate the difference. If the electron stays in the bubble during the density increase, it experiences higher electric field in the rear part of the bubble again. In such a case, electron energy and γ increase, and λ_b and r_β remain almost unchanged. These findings are also confirmed by the fact that observer receives signal almost at the same times but with different intensity.

On the other hand, if the rear part of the bubble precedes the electron, it can even slightly loose energy during the time spent there. However, the critical energy increases. Looking at the trajectory of such an electron, it can be seen that the amplitude of oscillations increases and λ_β decreases. Also, signals from such an electron are detected at different times with different intensities. Despite the fact that overall increase in the energy of such electrons is small compared to the previous case, it seems that an amplitude growth contributes to the critical frequency increase.

The increase in amplitude can be explained as follows. If the electron is at the upper part of the bubble, it experiences negative transverse force. As a consequence, the electron is pushed back to the bottom part. Similarly, when the electron is at the bottom part, it is pushed back upward, which induces transverse oscillations.

However, if the electron occurs behind the bubble, transverse force changes its sign (see Figure 6). For instance, if the electron is originally above the axis ($y > 0$), it suddenly occurs at the positive transverse force region behind the bubble and is pushed upward for a longer time, and vice versa. This behaviour enforces stronger oscillations. After that, the bubble elongates again and the electron occurs at the rear part of the bubble with a significantly higher amplitude of oscillations. Such an amplitude boost is also apparent in the energy distribution of back electrons in Figure 3.

5. CONCLUSION

Manipulation with plasma density profile is a promising way of enhancing betatron radiation in LWFA. Results presented in this paper indicate that the value of critical energy can be increased more than five times by using a properly designed up-ramp. Our simulations show two possible ways of improvement: either by electron energy gain in the rear part of the bubble or by oscillation amplitude boost by fields behind the bubble. These findings suggest that properties of the betatron radiation are very sensitive to the position of electrons in the bubble. Therefore, there is abundant room for further research in the betatron radiation generation by tailoring the plasma density. Such a research may lead to better understanding of the process and improved design of accelerators for practical applications.

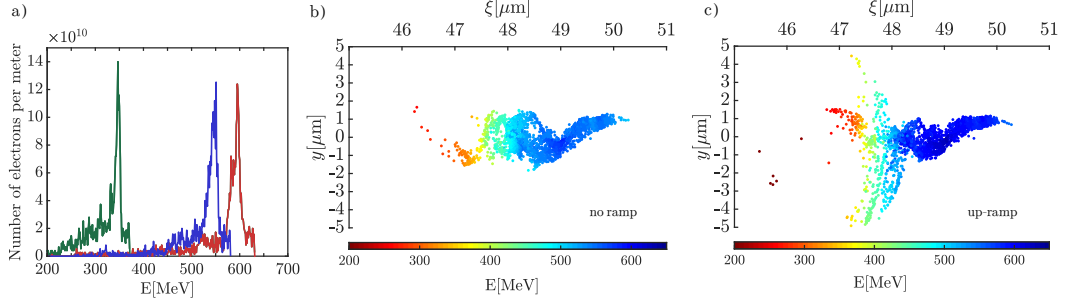


Figure 3: a) Electron energy spectrum in 0.9 mm of pulse propagation (green) and in 1.5 mm of pulse propagation through uniform density (blue) and linear density up-ramp (red). Energy distribution of electrons in ξ - y -plane in 1.5 mm of pulse propagation are shown for b) uniform density profile c) density profile with a linear up-ramp. ξ is a co-moving coordinate with the pulse.

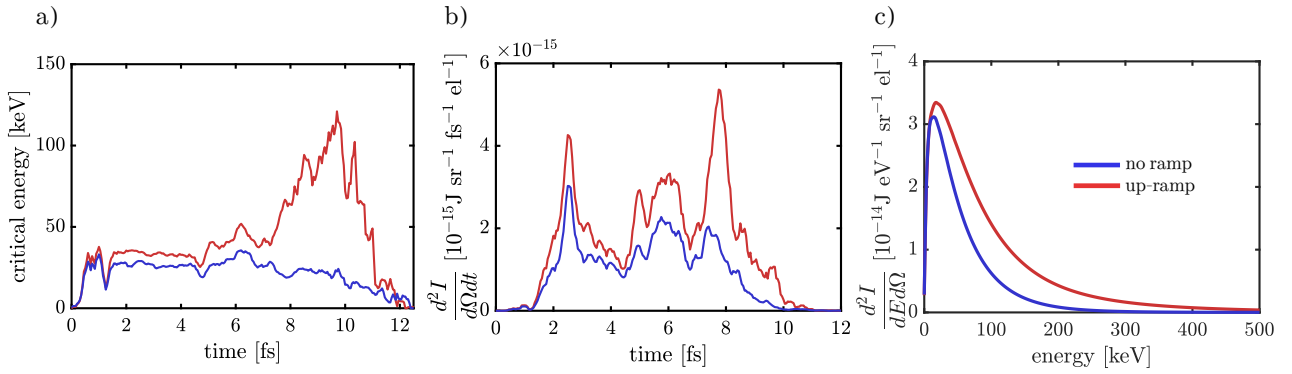


Figure 4: a) Temporal evolution of critical energy, b) temporal profile of radiative power and c) spectrum on axis in 1.5 mm of pulse propagation with two different density profiles: uniform density (blue), density profile with a linear up-ramp (red).

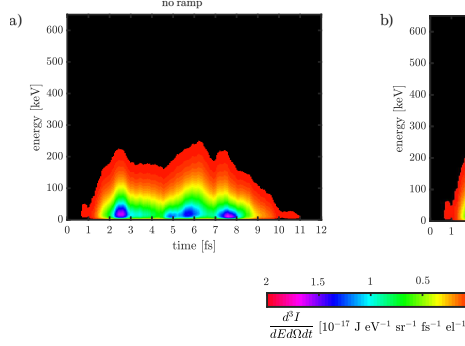


Figure 5: Spectrograms of betatron radiation in 1.5 mm of acceleration for a) uniform density profile, b) density profile with a linear up-ramp.

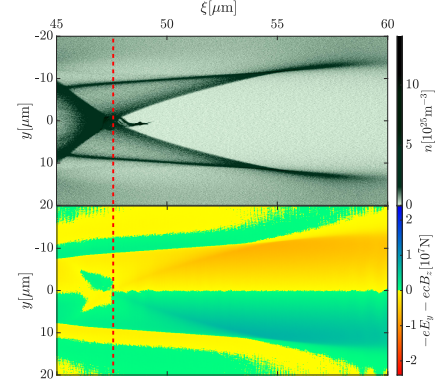


Figure 6: Density profile of the bubble and transverse Lorentz force in 1.35 mm of pulse propagation. The dashed line shows the beginning of the bubble. ξ is a co-moving coordinate with the pulse.

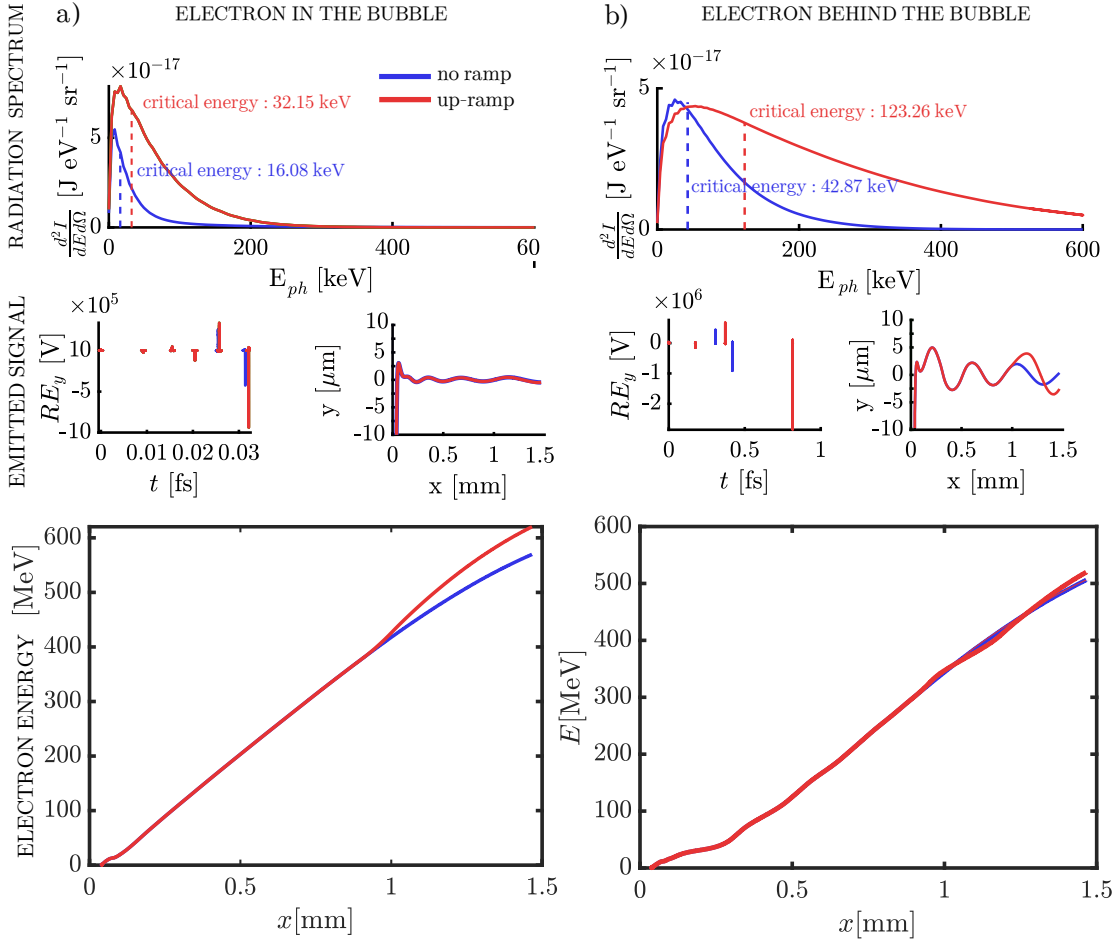


Figure 7: Betatron radiation properties of two example electrons in 1.5 mm of pulse propagation originally trapped a) in the bubble b) behind the bubble for two density profiles: uniform density (blue), a linear upramp (red). First row: radiated photon energy E_{ph} spectrum on axis. Second row: Radiation signal $E_y(t)R(t)$ (left) from the peaks of sinusoidal trajectory in xy -plane (right). Third row: Evolution of electron energy during acceleration.

ACKNOWLEDGMENTS

Computational resources were provided by The Ministry of Education, Youth and Sports from the Large Infrastructures for Research, Experimental Development and Innovations project "IT4Innovations National Supercomputing Center – LM2015070". Access to computing and storage facilities owned by parties and projects contributing to the National Grid Infrastructure MetaCentrum provided under the programme "Projects of Large Research, Development, and Innovations Infrastructures" (CESNET LM2015042), is greatly appreciated. The work was partially supported from European Regional Development Fund - Project "Center for Advanced Applied Science" (No. CZ.02.1.01/0.0/0.0/16_019/0000778) and Project "Creating and probing dense plasma at the PALS facility" (No. CZ.02.1.01/0.0/0.0/16_013/0001552).

REFERENCES

- [1] Kneip, S., McGuffey, C., Martins, J., Martins, S., Bellei, C., Chvykov, V., Dollar, F., Fonseca, R., Huntington, C., Kalintchenko, G., et al., "Bright spatially coherent synchrotron X-rays from a table-top source," *Nature Physics* **6**(12), 980 (2010).
- [2] Hogan, M. J., Assmann, R., Decker, F.-J., Iverson, R., Raimondi, P., Rokni, S., Siemann, R., Walz, D., Whittum, D., Blue, B., et al., "E-157: A 1.4-m-long plasma wake field acceleration experiment using a 30 GeV electron beam from the stanford linear accelerator center linac," *Physics of Plasmas* **7**(5), 2241–2248 (2000).
- [3] Esarey, E., Shadwick, B., Catravas, P., and Leemans, W., "Synchrotron radiation from electron beams in plasma-focusing channels," *Physical Review E* **65**(5), 056505 (2002).
- [4] Kostyukov, I., Kiselev, S., and Pukhov, A., "X-ray generation in an ion channel," *Physics of Plasmas* **10**(12), 4818–4828 (2003).
- [5] Rousse, A., Phuoc, K. T., Shah, R., Pukhov, A., Lefebvre, E., Malka, V., Kiselev, S., Burg, F., Rousseau, J.-P., Umstadter, D., et al., "Production of a keV X-ray beam from synchrotron radiation in relativistic laser-plasma interaction," *Physical review letters* **93**(13), 135005 (2004).
- [6] Kostyukov, I., Pukhov, A., and Kiselev, S., "Phenomenological theory of laser-plasma interaction in "bubble" regime," *Physics of Plasmas* **11**(11), 5256–5264 (2004).
- [7] Lu, W., Huang, C., Zhou, M., Tzoufras, M., Tsung, F., Mori, W., and Katsouleas, T., "A nonlinear theory for multidimensional relativistic plasma wave wakefields," *Physics of Plasmas* **13**(5), 056709 (2006).
- [8] Jackson, J. D., [Classical electrodynamics], John Wiley & Sons (2007).
- [9] Michel, P., Schroeder, C., Shadwick, B., Esarey, E., and Leemans, W., "Radiative damping in plasma-based accelerators," in [AIP Conference Proceedings], **877**(1), 554–560, AIP (2006).
- [10] Phuoc, K. T., Corde, S., Shah, R., Albert, F., Fitour, R., Rousseau, J.-P., Burg, F., Mercier, B., and Rousse, A., "Imaging electron trajectories in a laser-wakefield cavity using betatron X-ray radiation," *Physical review letters* **97**(22), 225002 (2006).
- [11] Kneip, S., Nagel, S., Bellei, C., Bourgeois, N., Dangor, A., Gopal, A., Heathcote, R., Mangles, S., Marques, J., Maksimchuk, A., et al., "Observation of synchrotron radiation from electrons accelerated in a petawatt-laser-generated plasma cavity," *Physical review letters* **100**(10), 105006 (2008).
- [12] Mangles, S., Genoud, G., Kneip, S., Burza, M., Cassou, K., Cros, B., Dover, N., Kamperidis, C., Najmudin, Z., Persson, A., et al., "Controlling the spectrum of x-rays generated in a laser-plasma accelerator by tailoring the laser wavefront," *Applied Physics Letters* **95**(18), 181106 (2009).
- [13] Nemeth, K., Shen, B., Li, Y., Shang, H., Crowell, R., Harkay, K. C., and Cary, J. R., "Laser-driven coherent betatron oscillation in a laser-wakefield cavity," *Physical review letters* **100**(9), 095002 (2008).
- [14] Mangles, S. P., Thomas, A. G. R., Kaluza, M., Lundh, O., Lindau, F., Persson, A., Tsung, F., Najmudin, Z., Mori, W. B., Wahlström, C.-G., et al., "Laser-wakefield acceleration of monoenergetic electron beams in the first plasma-wave period," *Physical review letters* **96**(21), 215001 (2006).
- [15] Cipiccia, S., Islam, M. R., Ersfeld, B., Shanks, R. P., Brunetti, E., Vieux, G., Yang, X., Issac, R. C., Wiggins, S. M., Welsh, G. H., et al., "Gamma-rays from harmonically resonant betatron oscillations in a plasma wake," *Nature Physics* **7**(11), 867 (2011).
- [16] Popp, A., Vieira, J., Osterhoff, J., Major, Z., Hörlein, R., Fuchs, M., Weingartner, R., Rowlands-Rees, T. P., Marti, M., Fonseca, R. A., Martins, S. F., Silva, L. O., Hooker, S. M., Krausz, F., Grüner, F., and Karsch, S., "All-optical steering of laser-wakefield-accelerated electron beams," *Phys. Rev. Lett.* **105**, 215001 (Nov 2010).
- [17] Chen, L., Yan, W., Li, D., Hu, Z., Zhang, L., Wang, W., Hafz, N., Mao, J., Huang, K., Ma, Y., et al., "Bright betatron X-ray radiation from a laser-driven-clustering gas target," *Scientific reports* **3**, 1912 (2013).
- [18] Wood, J., Poder, K., Lopes, N., Cole, J., Alatabi, S., Kamperidis, C., Mangles, S., Sahai, A., Najmudin, Z., Kononenko, O., et al., "Enhanced betatron radiation from a laser wakefield accelerator in a long focal length geometry," *Gas* **1**(3), 2.
- [19] Yan, W., Chen, L., Li, D., Zhang, L., Hafz, N. A., Dunn, J., Ma, Y., Huang, K., Su, L., Chen, M., et al., "Concurrence of monoenergetic electron beams and bright X-rays from an evolving laser-plasma bubble," *Proceedings of the National Academy of Sciences* , 201404336 (2014).

- [20] Ferri, J. and Davoine, X., "Enhancement of betatron x rays through asymmetric laser wakefield generated in transverse density gradients," *Physical Review Accelerators and Beams* **21**(9), 091302 (2018).
- [21] Ma, Y., Seipt, D., J. D. Dann, S., Streeter, M., Palmer, C., Willingale, L., and Thomas, A., "Angular streaking of betatron X-rays in a transverse density gradient laser-wakefield accelerator," *Physics of Plasmas* **25**, 113105 (11 2018).
- [22] Ta Phuoc, K., Esarey, E., Leurent, V., Cormier-Michel, E., Geddes, C., Schroeder, C., Rousse, A., and Leemans, W., "Betatron radiation from density tailored plasmas," *Physics of Plasmas* **15**(6), 063102 (2008).
- [23] Döpp, A., Guillaume, E., Thaury, C., Lifschitz, A., Ta Phuoc, K., and Malka, V., "Energy boost in laser wakefield accelerators using sharp density transitions," *Physics of Plasmas* **23**(5), 056702 (2016).
- [24] Guo, B., Zhi, C., Liu, S., Nan Ning, X., Zhang, J., Pai, C.-H., Hua, J., Chu, H.-H., Wang, J., and Lu, W., "Enhancement of laser-driven betatron X-rays by a density-depressed plasma structure," *Plasma Physics and Controlled Fusion* (12 2018).
- [25] Arber, T., Bennett, K., Brady, C., Lawrence-Douglas, A., Ramsay, M., Sircombe, N., Gillies, P., Evans, R., Schmitz, H., Bell, A., et al., "Contemporary particle-in-cell approach to laser-plasma modelling," *Plasma Physics and Controlled Fusion* **57**(11), 113001 (2015).
- [26] Horný, V., Petržílka, V., Klímo, O., and Krůš, M., "Short electron bunches generated by perpendicularly crossing laser pulses," *Physics of Plasmas* **24**(10), 103125 (2017).
- [27] Horný, V., Mašlárová, D., Petržílka, V., Klímo, O., Kozlová, M., and Krůš, M., "Optical injection dynamics in two laser wakefield acceleration configurations," *Plasma Physics and Controlled Fusion* **60**(6), 064009 (2018).
- [28] Horný, V., Nejdl, J., Kozlová, M., Krůš, M., Boháček, K., Petržílka, V., and Klímo, O., "Temporal profile of betatron radiation from laser-driven electron accelerators," *Physics of Plasmas* **24**(6), 063107 (2017).